Fluorescence microscopy in a microwave cavity

Michael J. R. Previte and Chris D. Geddes*

Institute of Fluorescence, Laboratory for Advanced Medical Plasmonics, Medical Biotechnology Center, University of Maryland Biotechnology Institute, 725 West Lombard St., Baltimore, MD, 21201.
**Corresponding author: geddes@umbi.umd.edu*

Abstract: Optical microscopy is a well-established technique that has wide ranging applications for imaging molecular dynamics of biological systems. Typically, these applications rely on external temperature controllers to maintain or change reactions rates of these biological systems. With increasing interest in applying low power microwaves to drive biological and chemical reactions, we have combined optical and microwave based technologies and developed a fluorescence microscope in a microwave cavity. With this instrument, we have found a means to optically image biological systems inside microwave cavities during the application of microwave pulses.

OCIS codes: (110.0180) Microscopy; (180.2520) Fluorescence Microscopy; (300.6370) Spectroscopy, fluorescence and luminescence; (300.6370) Spectroscopy, microwave; (350.4010) Microwaves

References and links

1. S. Haduch, S. Baranski, and P. Czerski, "Effect of microwave radiations on the human organism," Acta physiologica Polonica **11**, 717-719 (1960).
2. S. Baranski, L. Czekalinski, P. Czerski, and S. Haduch, "Experimental research on the fatal effect of micrometric wave irradiation," Revue de medecine aeronautique **2**, 108-111 (1963).
3. Z. Bielicki, S. Baranski, P. Czerski, and S. Haduch, "Analysis of difficulties of occupational activity in personnel exposed to micrometric wave irradiation," Revue de medecine aeronautique **2**, 106-107 (1963).
4. S. Baranski and Z. Edelwejn, "Experimental morphologic and electroencephalographic studies of microwave effects on nervous system," Annals of the New York Academy of Sciences **247**, 109-116 (1975).
5. E. H. Grant, R. J. Sheppard, and G. P. South, *Dielectric Behavior of Biological Molecules in Solution* (Oxford University Press, 1978).
6. A. W. J. Dawkins, N. R. V. Nightingale, G. P. South, R. J. Sheppard, and E. H. Grant, "Role of water in microwave-absorption by biological-material with particular reference to microwave hazards," Phys. Med. Biol. **24**, 1168-1176 (1979).
7. S. Takashima, C. Gabriel, R. Sheppard, and E. Grant, "Dielectric behavior of DNA solution at radio and microwave frequencies (at 20 degrees C)," Biophys. J. **46**, 29-34 (1984).
8. I. Roy and M. N. Gupta, "Applications of microwaves in biological sciences," Curr. Sci. **85**, 1685-1693 (2003).
9. S. Jain, S. Sharma, and M. N. Gupta, "A microassay for protein determination using microwaves," Anal. Biochem. **311**, 84-86 (2002).
10. H. Bohr and J. Bohr, "Microwave-enhanced folding and denaturation of globular proteins," Phys. Rev. E **61**, 4310-4314 (2000).
11. K. R. Foster, "Thermal and nonthermal mechanisms of interaction of radio-frequency energy with biological systems," IEEE Trans. Plasma Sci. **28**, 15-23 (2000).
12. K. Hamad-Schifferli, J. J. Schwartz, A. T. Santos, S. G. Zhang, and J. M. Jacobson, "Remote electronic control of DNA hybridization through inductive coupling to an attached metal nanocrystal antenna," Nature **415**, 152-155 (2002).
13. M. Zimmer, "Green fluorescent protein (GFP): Applications, structure, and related photophysical behavior," Chemical Reviews **102**, 759-781 (2002).
14. A. B. Copty, Y. Neve-Oz, I. Barak, M. Golosovsky, and D. Davidov, "Evidence for a specific microwave radiation effect on the green fluorescent protein," Biophys. J. **91**, 1413-1423 (2006).
15. M. J. R. Previte, and C. D. Geddes, "Microwave-triggered chemiluminescence with planar geometrical aluminum substrates: Theory, simulation and experiment," J. Fluoresc. **17**, 279-287 (2007).
16. K. Aslan, S. N. Malyn, and C. D. Geddes, "Microwave-accelerated surface plasmon coupled directional luminescence: Application to fast and sensitive assays in buffer, human serum and whole blood," J. Immunol. Methods **323**, 55-64 (2007).
17. K. Aslan, and C. D. Geddes, "Microwave-accelerated metal-enhanced fluorescence: Platform technology for ultrafast and ultrabright assays," Anal. Chem. **77**, 8057-8067 (2005).

#83953 - $15.00 USD Received 8 Jun 2007; revised 16 Aug 2007; accepted 23 Aug 2007; published 29 Aug 2007

18. K. Aslan, S. N. Malyn, and C. D. Geddes, "Fast and sensitive DNA hybridization assays using microwave-accelerated metal-enhanced fluorescence," Biochem. and Biophys. Res. Comm. **348**, 612-617 (2006).
19. V. Sridar, "Rate acceleration of Fischer-indole cyclization by microwave irradiation," Indian J. Chem. **36**, 86-87 (1997).
20. "Technology Vision 2020," (The U.S. Chemical Industry, 1996).
21. V. Sridar, "Microwave radiation as a catalyst for chemical reactions," Curr. Sci. **74**, 446-450 (1998).
22. R. S. Varma, "Advances in Green chemistry: Chemical Synthesis using microwave irradiation," (Astrazeneca Research Foundation, India, Banglore, 2002).
23. C. O. Kappe, "High-speed combinatorial synthesis utilizing microwave irradiation," Curr. Opin. Chem. Biol. **6**, 314-320 (2002).
24. D. Adam, "Microwave chemistry: Out of the kitchen," Nature **421**, 571-572 (2003).
25. K. Aslan, S. N. Malyn, and C. D. Geddes, "Multicolor microwave-triggered metal-enhanced chemiluminescence," J. Am. Chem. Soc. **128**, 13372-13373 (2006).
26. R. S. Varma, "Solvent-free organic syntheses - using supported reagents and microwave irradiation," Green Chemistry **1**, 43-55 (1999).
27. R. Gedye, F. Smith, K. Westaway, H. Ali, L. Baldisera, L. Laberge, and J. Rousell, "The use of microwave-ovens for rapid organic-synthesis," Tetrahedron Lett. **27**, 279-282 (1986).
28. A. G. Whittaker, and D. M. P. Mingos, "Microwave-assisted solid-state reactions involving metal powders," J. Chem. Soc. Dalton Trans. **12**, 2073-2079 (1995).
29. S. Caddick, "Microwave assisted organic reactions," Tetrahedron **51**, 10403-10432 (1995).
30. M. Pagnotta, C. L. F. Pooley, B. Gurland, and M. Choi, "Microwave activation of the mutarotation of alpha-D-glucose – an example of an intrinsic microwave effect," J. Phys. Org. Chem. **6**, 407-411 (1993).
31. A. Shaman, S. Mizrahi, U. Cogan, and E. Shimoni, "Examining for possible non-thermal effects during heating in a microwave oven," Food Chemistry **103**, 444-453 (2007).
32. R. K. Adair, "Biophysical limits on athermal effects of RF and microwave radiation," Bioelectromagnetics **24**, 39-48 (2003).
33. R. Weissenborn, K. Diederichs, W. Welte, G. Maret, and T. Gisler, "Non-thermal microwave effects on protein dynamics? An X-ray diffraction study on tetragonal lysozyme crystals," Acta Crystallogr. **61**, 163-172 (2005).
34. J. Gellermann, W. Wlodarczyk, B. Hildebrandt, H. Ganter, A. Nicolau, B. Rau, W. Tilly, H. Fahling, J. Nadobny, R. Felix, and P. Wust, "Noninvasive magnetic resonance thermography of recurrent rectal carcinoma in a 1.5 Tesla hybrid system," Cancer Res. **65**, 5872-5880 (2005).
35. M. J. R. Previte, and C. D. Geddes, "Spatial and temporal control of microwave triggered chemiluminescence: A rapid and sensitive protein detection platform," Anal. Chem. **in press** (2007).
36. C. L. R. Catherall, T. F. Palmer, and R. B. Cundall, "Chemiluminescence from reactions of bis(Pentachrlophenyl)oxalate, hydrogen-peroxide and fluorescent compounds – kinetics and mechanism," J. Chem. Soc. Faraday Trans. Trans 11 **80**, 823-836 (1984).
37. O. Filevich, and R. Etchenique, "1D and 2D temperature imaging with a fluorescent ruthenium complex," Anal. Chem. **78**, 7499-7503 (2006).
38. B. Durham, J. V. Caspar, J. K. Nagle, and T. J. Meyer, "Photochemistry of $Ru(bpy)_3^{2+}$," J. Am. Chem. Soc. **104**, 4803-4810 (1982).
39. J. Vanhouten and R. J. Watts, "Temperature-dependence of photophysical and photochemical properties of Tris(2,2'-bypridyl)Ruthenium(II) ion in aqueous solution," J. Am. Chem. Soc. **98**, 4853-4858 (1976).
40. O. Filevich, and R. Etchenique, "1D and 2D temperature imaging with a fluorescent ruthenium complex," Anal. Chem. **78**, 7499-7503 (2006).
41. N. A. Nemkovich, A. N. Rubinov, and A. T. Tomin, "Inhomogeneous Broadening of Electronic Spectra of Dye Molecules in Solutions," in *Topics in Fluorescence Spectroscopy, Vol. 2, Principles*, J. R. Lakowicz, ed., (Plenum Press, New York, 1991), pp. 367-428.

1. Introduction

Historically, the study of the application of microwaves to biological systems has drawn interest with regards to the hazards of prolonged exposure to microwave irradiation [1-7]. Since prolonged exposure to microwave irradiation has been considered deleterious to biological systems and biomolecules, the general applicability of microwave technology to biological studies has been limited [8]. As a result, combining microscopy and microwave technology is a concept that had limited practical relevance.

Recently, more practical applications of microwave irradiation for biological studies have been reported [8-18]. While microwaves have been shown to accelerate the rate of chemical reactions [19-25] and enzyme-catalyzed biological reactions [8, 9, 24, 26, 27] some argue that the enhanced reaction rates in many microwave assisted reactions cannot be explained by heating alone. It has been suggested that there exists a "non-thermal" effect on biological systems, which potentially permutes enzyme, DNA and protein function and conformation after microwave exposure [14, 24, 28-31]. Recent works summarize some existing theories

#83953 - $15.00 USD Received 8 Jun 2007; revised 16 Aug 2007; accepted 23 Aug 2007; published 29 Aug 2007

with regard to the interactions of microwaves with biological systems [11, 32, 33], but many of these works describe the before and after effects of microwaves on biological systems with a few exceptions [10, 12, 14, 34].

The recent published work by Copty, *et al*. studied microwave effects on green fluorescent protein (GFP) in real-time [14]. To perform related studies and address the need for real-time data of microwave effects on biological processes, a real-time imaging system could greatly facilitate the understanding of microwave effects on enzyme reactions rates, biomolecular interactions, and living biological organisms, i.e. mammalian cells. We use technologies developed in our laboratory to demonstrate the development of a real-time fluorescence imaging system in a microwave cavity. With this instrument, we introduce a means to record real-time data of biomolecule interactions and biological systems inside microwave cavities during the application of a microwave field.

2. Materials

Premium quality APS-coated glass slides (75x25 mm) were obtained from Sigma-Aldrich. CoverWell imaging chamber gaskets with adhesive (2.5 mm diameter, 2 mm deep and 5 mm diameter, 2 mm deep for temperature measurements) were obtained from Molecular Probes (Eugene, OR). $Ru(by)_2Cl_2$ salt was obtained from Sigma-Aldrich. Commercially available chemiluminescence materials were purchased from Unique Industries, Inc.

3. Methods

3.1 Optical set-up of wide-field microscope in microwave cavity

At the base and center of the microwave cavity (0.7 cu ft, GE Compact Microwave Model: JES735BF, max power 700W), we removed a DC motor and spindle apparatus, which was used to rotate a turntable, from a ½" aperture. This aperture was widened to 1 inch to allow the objective to sit in the cavity and subsequent exposed metal surfaces were covered with white enamel paint to prevent sparking and arcing. With the widened aperture, any subsequent leakage of microwave radiation from the cavity was not significant enough to create a measurable temperature change to a 10 ml volume of water that was positioned approximately 3 cm below the center of the aperture. For safety, the optical configuration was shielded by aluminum sheets to minimize exposure to microwave radiation.

Using a beam expander, the spot size of a 473 nm laser source was expanded to approximately 1 inch and focused at the back aperture of the objective with a tube lens (FL = 175 mm). The incident excitation beam was reflected with a dichroic mirror (z479/532rpc, Chroma, Brattleboro, VT) into an infinity corrected brightfield objective (LWD Plan Achromat objective -LPL10 x objective/NA = .25). The fluorescent emission intensity, which is generated by wide-field excitation working in epifluorescence mode, is collected through the infinity corrected optics and imaged onto a CCD camera using a razor edge 488 nm and a 570 LP filter to block any bleedthrough of the excitation light (Fig. 1). Chemiluminescence intensity images are imaged through the infinity corrected optics and imaged onto a CCD camera in the absence of any optical filters.

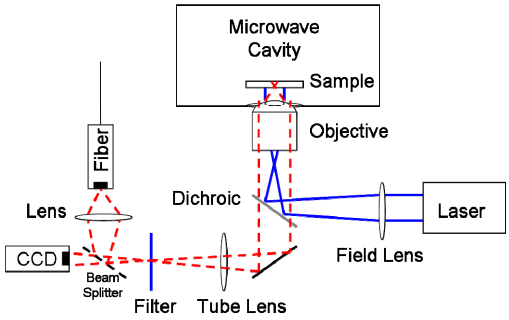

Fig. 1. Optical scheme of a wide-field microscope in a microwave cavity.

#83953 - $15.00 USD Received 8 Jun 2007; revised 16 Aug 2007; accepted 23 Aug 2007; published 29 Aug 2007

CCD images were taken with a Retiga-SRV CCD Camera (QImaging, Burnaby, B.C.) with 4x4 binning at 10 fps. Emission spectra were collected using an Ocean Optics spectrometer, model SD 2000 (Dunedin, FL) that is connected to an Ocean Optics 1000 μm diameter fiber with a NA of 0.22 (Dunedin, FL). A collimator is connected to the end of the fiber and positioned to maximize the coupling of the fluorescence emission into the spectrometer (Fig. 1). $Ru(by)_2Cl_2$ time-dependent emission spectra were collected with an integration time of 100 milliseconds.

All exposed metal surfaces of the objective and adaptive optics were coated with white reflective paint to prevent sparking and arcing during the application of microwave pulses.

3.2 Formation of continuous metal films on APS-coated glass substrates

The preparation of glass slides modified with 'bow-tie' structures has been described previously [35]. Briefly, disjointed 'bow-tie' equilateral 2.5 mm triangles stencils were made from an adhesive mask. The disjointed 'bow-tie' structure was formed from two inverted 5 mm triangles, such that the distance between the apexes or gap size was approximately 2-3 mm (Fig. 2). Triangle tape masks were affixed to plain glass slides and glass slides modified with Ag triangle structures were created by vapor depositing 75 nm of Au films on glass using an EMF Corp. (Ithaca, NY) vapor deposition instrument (Fig. 2).

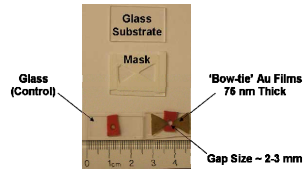

Fig. 2. Sample geometry scheme.

Film thicknesses were monitored during the deposition process with an Edwards FTM6 film thickness monitor.

3.3 Sample preparation

Glass substrates with and without modified 'bow-tie' metal structures were cut into 10 x 10 mm sample sizes. Image wells were placed between the two vapor deposited Au triangles 75 nm thick or at the 'bowtie' gap and on the unmodified plain glass substrates. The samples were subsequently filled with 20 μl of 10 μM $Ru(by)_2Cl_2$ solution or 6 μl of chemiluminescence material (Fig. 2.).

3.4 Chemiluminescence reagents (chemical reaction assays)

The commercially available glow-sticks contain a phenyl oxalate ester, a fluorescent probe and a glass capsule containing the activating agent (hydrogen peroxide). Activation of the chemicals is accomplished by breaking an encapsulated glass capsule that contains the peroxide and subsequently mixes the chemicals to begin the chemiluminescence reaction. The hydrogen peroxide oxidizes the phenyl oxalate ester to a peroxyacid ester and phenol [36]. The unstable peroxyacid ester decomposes to a peroxy compound and phenol, the process chemically inducing an electronic excited state [36].

3.5 $Ru(by)_2Cl_2$ temperature measurements

Previously, ruthenium chloride aqueous solutions have been used to calibrate a temperature imaging system with a CCD sensor [37]. The temperature dependence of the photophysical and photochemical properties of ruthenium chloride aqueous solutions have been described in detail elsewhere [38, 39]. Since the emission intensity of these solutions linearly decrease with temperature, a pre-calibrated intensity vs. temperature plot of a 10 μM aqueous solutions of $Ru(by)_2Cl_2$ was recorded using a Cary Eclipse fluorescence spectrometer with temperature

#83953 - $15.00 USD Received 8 Jun 2007; revised 16 Aug 2007; accepted 23 Aug 2007; published 29 Aug 2007

controller (Fig. 3). Calibration temperatures were 10, 20, 30, 40, 50, 60, and 70 °C, which is within the linear range of the relationship between the relative fluorescence to the temperature (Fig. 3) [37].

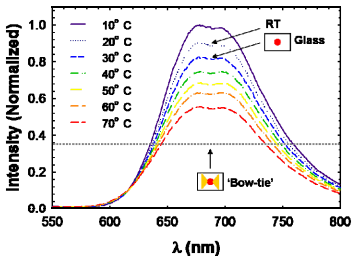

Fig. 3. Normalized intensity spectra for 10 μM $Ru(by)_2Cl_2$ at different temperatures. Normalized intensity ratios of 10 μM $Ru(by)_2Cl_2$ solutions are marked with an arrow for the glass geometry (inset, sample geometry) and a dotted line for the 'bow-tie' sample geometries (inset, sample geometry). Normalized intensity ratios are calculated as the ratio of the time dependent emission intensity during to the maximum emission intensity before exposure to short microwave pulse.

For the microwave imaging experiments, the intensity of fluorescence emission was measured from 10 μM aqueous solutions of $Ru(by)_2Cl_2$ on glass substrates in the presence and absence of the thin continuous metal film triangle geometries 75 nm thick (Fig. 3). $Ru(by)_2Cl_2$ aqueous solutions were excited with a 473 nm laser source. Before and during the application of a 5 second low power 2.45 GHz microwave pulses (10% power), the spectral emission from the $Ru(by)_2Cl_2$ aqueous solutions was recorded at 100 millisecond time intervals for 20 seconds using the fiber detection and spectrometer optical configuration (Fig. 1). The recorded fluorescence spectral intensity from the $Ru(by)_2Cl_2$ aqueous solutions on glass substrates and 'bow-tie' modified substrates before and during the application of the microwave pulse were normalized (Fig. 4). The normalized spectra are superimposed to determine if the microwave fields induce any spectral change to the $Ru(by)_2Cl_2$ emission (Fig. 4). The CCD time dependent intensities are normalized with respect to the maximum emission intensity (time = 0). Normalized intensity ratios are calculated as the ratio of the time dependent emission intensity to the maximum emission intensity before exposure to short microwave pulse. Subsequently, these ratios multiplied by a factor of .9 (Fig 3, RT) to reflect the normalized intensity ratio for 10 μM aqueous solutions of $Ru(by)_2Cl_2$ at room temperature (Fig. 3). The corresponding temperature values for microwave heated solutions on glass substrates and substrates with 'bow-tie geometries could be approximated from the pre-calibrated intensity vs. temperature plot of a $Ru(by)_2Cl_2$ sample of the same concentration (Fig. 3, arrow and dashed line).

Total emission intensity images for $Ru(by)_2Cl_2$ aqueous solutions and chemiluminescence samples were captured at frame rate of 10 Hz using a CCD camera (Figs. 6-10). In order to obtain the same initial chemiluminescence emission for all measurements, approximately 6 μl of the chemiluminescence solution was placed inside the imaging chamber. Data collection commenced 10 seconds prior to the application of the five second microwave pulse and continued until 20 seconds after microwave exposure.

4. Results

Since it is well established that the emission intensity of $Ru(by)_2Cl_2$ solutions are inversely proportional to temperature, we recorded the emission spectra for $Ru(by)_2Cl_2$ solutions over a range of temperatures [40]. From these spectra, we observed a linear relationship between the emission intensity and temperature for the 10 μM $Ru(by)_2Cl_2$ solutions between 10 °C and 70 °C, which is consistent with previously published results (Fig. 3) [35]. Using the fiber detection configuration of the optical scheme (Fig. 1), we recorded the fluorescence intensity

#83953 - $15.00 USD Received 8 Jun 2007; revised 16 Aug 2007; accepted 23 Aug 2007; published 29 Aug 2007

from the $Ru(by)_2Cl_2$ aqueous solution at 100 millisecond time intervals for approximately 60 seconds. During the 60 second recording, we applied a five second 2.45 GHz pulse microwave pulse. Normalized intensity vs. temperature plots of the $Ru(by)_2Cl_2$ sample of the same concentration (Fig. 3) was fit to a linear function (data not shown). The approximate microwave induced maximum temperature increases to the solutions on the glass sample geometries is marked with an arrow, while the dashed line reflects the intensity decrease for the solution in the gap of the 'bow-tie' geometry (Fig. 3).

Although only part of the $Ru(by)_2Cl_2$ spectra is transmitted in the presence of the dichroic, the superimposed normalized intensity spectra of the $Ru(by)_2Cl_2$ before the application of a microwave pulse is shown (Fig. 4). Typically, spectral shifts in chromophore emission are ascribed to the changes in the electronic distribution of the energies of electronic transitions [41]. Since the normalized intensity spectra of $Ru(by)_2Cl_2$ solutions before the application of a microwave pulse (Fig. 4, black line) is not permuted during the application of a low power microwave pulse (Fig. 4, dotted and dashed lines), we concluded that the microwave heating does not create any noticeable change in the photophysical properties of the $Ru(by)_2Cl_2$ solutions [41].

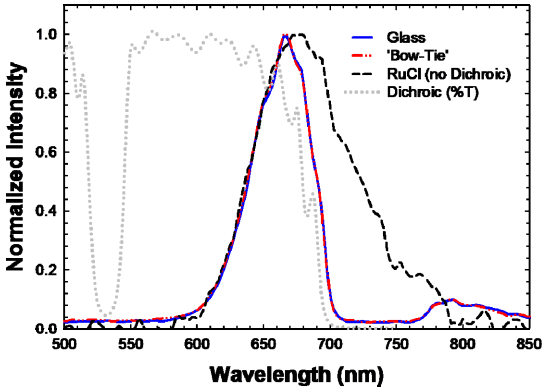

Fig. 4. Normalized spectra of $Ru(by)_2Cl_2$ emission (no dichroic) before (black dashed) and during the application of low power microwave pulses for 'bow-tie' (red dashed) and glass slide (blue dashed) sample geometries. Dichroic transmission curve is overlaid to show the filtering effect of the dichroic on $Ru(by)_2Cl_2$ emission (dotted gray line).

Using the CCD imaging configuration, we recorded the fluorescence intensity images of the $Ru(by)_2Cl_2$ aqueous solutions on the glass substrates with and without 'bow-tie' structures in the microwave cavity at a frame rate of 10 Hz for 10 seconds (Fig. 5).

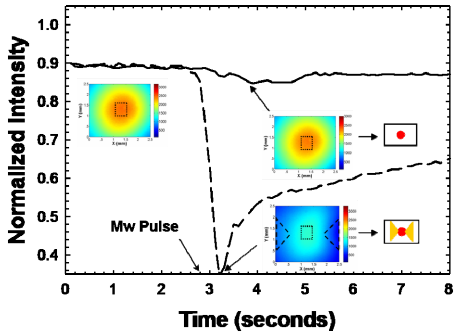

Fig. 5. The normalized average fluorescence intensity over 100 $pixel^2$ region (selected region approximated by box) time traces from CCD images for 10 μM $Ru(by)_2Cl_2$ solution at disjointed 'bow-tie' junction and on plain glass slides (control) during the application of 5 second low power microwave pulse (Mw pulse). Sample configurations are shown to the right of the CCD images. (insets)

#83953 - $15.00 USD Received 8 Jun 2007; revised 16 Aug 2007; accepted 23 Aug 2007; published 29 Aug 2007

During image collection, samples were exposed to five second microwave pulses. The pre-microwave fluorescence intensity is averaged over a 100 pixel^2 region selected from the center of the image (Fig. 5. insets, box outlines). The average intensity vs. time data of the CCD images for the 10 μM $Ru(by)_2Cl_2$ solution at disjointed 'bow-tie' junction and on plain glass slides (control) is normalized with respect to the maximum pre-microwave fluorescence intensity (Fig. 5) and scaled to the pre-calibrated room temperature normalized intensity (Fig. 3, 0.9 at RT). During exposure to the microwave pulse, we observed a slight decrease in the fluorescence intensity of the 10 μM $Ru(by)_2Cl_2$ solutions on the glass substrates, which corresponds to a temperature increase of about 5-8 °C (Fig. 5- top right, inset). On the other hand, we observed a significant decrease in the fluorescence intensity of the 10 μM $Ru(by)_2Cl_2$ solutions in the gap of a 'bow-tie' geometry during exposure to the microwave pulse (Fig. 5 - bottom right, inset), recalling that emission is inversely proportional to temperature. With respect to calibration curve of the 10 μM $Ru(by)_2Cl_2$ solutions intensity versus temperature, the temperature of the solutions on the glass substrate rose slightly above room temperature (Fig. 3, Glass), while the change in intensity of the 10 μM $Ru(by)_2Cl_2$ solutions in the gap of a 'bow-tie' geometry corresponds to a dramatic temperature decrease that is outside the linear range of the temperature versus intensity plot (Fig. 3, dashed line). These results are consistent with our previous report on the rapid heating of solutions with these 'bow-tie' structures [35]. Real time movies of the decrease in fluorescence intensity of these solutions during exposure to a low power microwave pulse are shown here to demonstrate the functionality of the fluorescence microscope in a microwave cavity [Figs. 6(A), 6(B)].

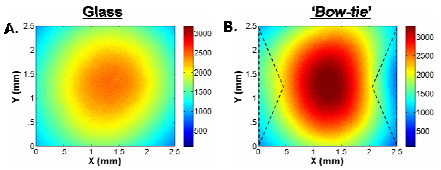

Fig. 6. The movies of the decrease in fluorescence intensity of 10 μM $Ru(by)_2Cl_2$ solutions during exposure to five second microwave pulse on A) plain glass substrates (2.3 MB) and B) on glass substrates modified with vapor deposited gold 'bow-tie' structures 75 nm thick (2.3 MB), demonstrate the functionality of the fluorescence microscope in a microwave cavity.

In addition to real-time imaging of temperature dependent $Ru(by)_2Cl_2$ solutions, we also imaged the local 'triggering' of chemiluminescent solutions to further validate the effectiveness of the microscope in a microwave concept. In our previous work, we have shown that it is possible to locally 'trigger' chemiluminescence reactions using vapor deposited geometric structures [15, 35]. We placed 6 μl of blue chemiluminescence solution in an imaging well affixed to plain glass substrates and in the 2 mm gap of the continuous gold thin film bow-tie' geometry [15, 35]. We recorded the chemiluminescence emission over at a frame rate of 10 Hz for 10 seconds (Fig. 7). During the 10 second time interval, samples were exposed to a five second microwave pulse, which induces the 'triggered' emission or dramatic rise in the maximum photon flux (Fig. 7).

#83953 - $15.00 USD Received 8 Jun 2007; revised 16 Aug 2007; accepted 23 Aug 2007; published 29 Aug 2007

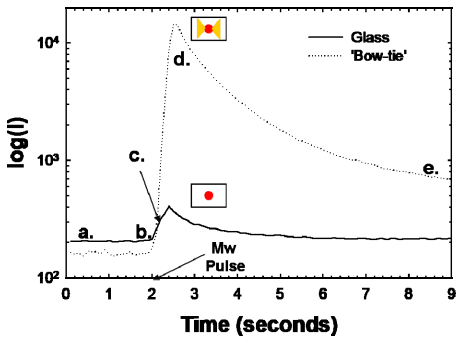

Fig. 7. Maximum pixel intensity time traces from chemiluminescent solutions on plain glass slides (control) and in the gap of a disjointed 'bow-tie' geometry 75 nm thick. CCD images are collected at a rate of 10 Hz for approximately 10 seconds. Samples are exposed to five second microwave pulses (Mw pulse) that are initiated approximately 2 seconds after data collection. Discrete time intervals are labeled as a) 0 seconds or steady state emission b) emission upon initial exposure to microwave pulse c) during the application of the microwave pulse d) maximum 'triggered' emission and e) final emission intensity.

Discrete time points are labeled and correspond to a) steady state emission b) emission upon initial exposure to microwave pulse c) during the onset of microwave pulse d) maximum 'triggered' emission during pulse and e) final chemiluminescence emission. During recording of the disjointed 'bow-tie' geometries intensity images, the CCD camera gain was decreased by about a factor of 4.5 to prevent saturation. Subsequently, the resulting CCD pixel intensities for the 'bow-tie' geometry are scaled accordingly to derive an absolute comparison to recorded chemiluminescence intensities from the glass substrates. CCD images of the chemiluminescence emission at these discrete time points are shown for the plain glass substrates (Fig. 8) and at the disjointed 'bow-tie junction (Fig. 9).

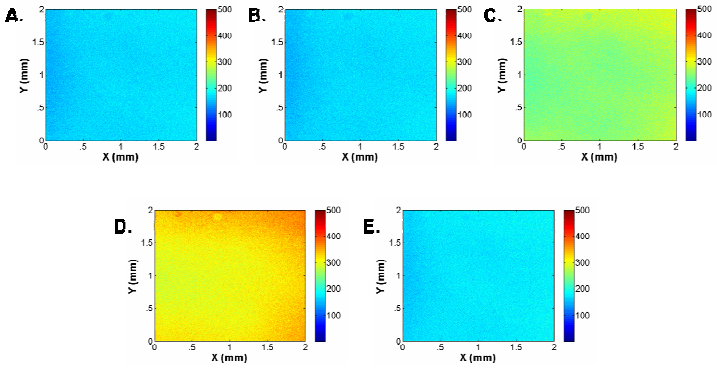

Fig. 8. CCD images of chemiluminescent solutions on plain glass slides (control) at discrete time intervals. CCD images are collected at a rate of 10 Hz for approximately 10 seconds. Samples are exposed to five second microwave pulses (Mw pulse) that are initiated approximately 2 seconds after data collection. Discrete time intervals are labeled as A) 0 seconds or steady state emission B) emission upon initial exposure to microwave pulse C) during the application of the microwave pulse D) maximum 'triggered' emission and E) final emission intensity.

#83953 - $15.00 USD Received 8 Jun 2007; revised 16 Aug 2007; accepted 23 Aug 2007; published 29 Aug 2007

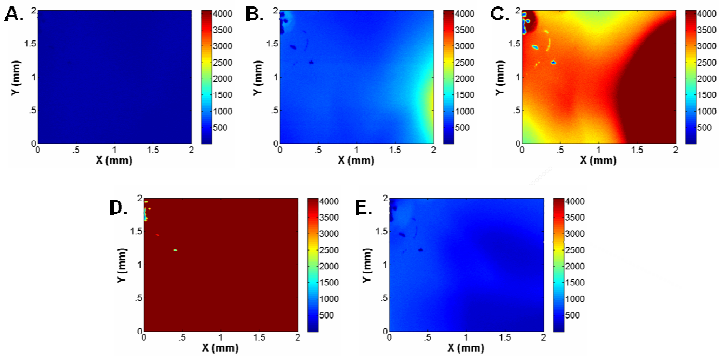

Fig. 9. CCD images of chemiluminescent solutions on disjointed 'bow-tie' junction at discrete time intervals. CCD images are collected at a rate of 10 Hz for approximately 10 seconds. Samples are exposed to five second microwave pulses (Mw pulse) that are initiated approximately 2 seconds after data collection. Discrete time intervals are labeled as A) 0 seconds or steady state emission B) emission upon initial exposure to microwave pulse C) during the application of the microwave pulse D) maximum 'triggered' emission and E) final emission intensity.

Pixel intensity scales for the both glass and 'bow-tie' images are equivalent to accurately reflect the dramatic increase in 'on-demand' photon flux from the chemiluminescent reactions. Again, real time movies of the increase in 'photon flux' from the chemiluminescence solutions during exposure to a low power microwave pulse are shown here to demonstrate the functionality of the fluorescence microscope in a microwave [Figs. 10(A), 10(B)].

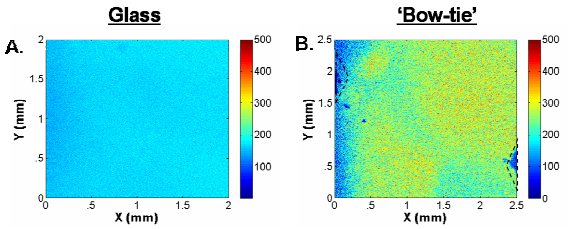

Fig. 10. CCD movie images for green for 6 µl of chemiluminescence solution A) on glass substrates (1.8 MB) and in the gap of B) disjointed 'bow-tie' geometries (2.3). Dashed outlines denote triangle 'bow-tie' tips.

5. Discussion

We have demonstrated the feasibility of constructing a fluorescence microscope in a microwave cavity. Using this optical configuration, we observed the microwave induced real-time temperature decreases in 10 µM $Ru(by)_2Cl_2$ solutions on plain glass substrates and in proximity to discrete planar structure geometries. Our results are consistent with our previous published reports of significant increases in heating rates of aqueous solutions in the presence of the planar metal geometries [35]. Although we did not detect any temperature rise in a sample of water proximal to the cavity aperture, we recognize that the modified cavity might still have resulted in minor microwave radiation loss that reduced the overall heating effect of the solutions. This is dually noted from the chemiluminescence emission results, whereby we observe approximately 100-fold increases in chemiluminescence emission from the 'bow-tie' geometry compared to the > 500-fold increases that were previously reported [35].

With regards to the 'triggering of the chemiluminescent reactions, the 'triggered' emission commences from the side that is closest to the incident microwave field generated by the magnetron. The CCD images of the chemiluminescent solutions depict the acceleration of the chemiluminescent reactions due to microwave heating or dielectric loss to the

#83953 - $15.00 USD Received 8 Jun 2007; revised 16 Aug 2007; accepted 23 Aug 2007; published 29 Aug 2007

chemiluminescence solution. Since the right side of the image [Fig. 9(B)] is oriented closest to the magnetron, we see the 'triggered' emission commence from the side closest to the microwave source. In a subsequent image [Fig. 9(C)], we observed the triggered emission from the wave reflected from the far wall of the cavity (Note: a standing wave is subsequently created in the cavity). It is important to note that the 'bow-tie' tips are slightly offset to facilitate the viewing of 'triggered' emission that results from reflected waves in a microwave cavity.

6. Conclusions

Using our existing microwave focused and triggering technologies, we have demonstrated the feasibility of capturing real-time images of microwave induced solution heating and accelerated chemiluminescence reactions. With the demonstration of the first *fluorescence microscope in a microwave cavity*, we believe that more complete analysis of the microwave effects on the interactions of biomolecules *in vitro* and *in vivo* is now possible. While we have demonstrated applications that are limited to the imaging of bulk solutions, work is currently underway to construct a confocal microscope that will allow us to perform single molecule experiments. Results will be published in due course.

Acknowledgments

The authors would like to acknowledge the IoF for salary support.

#83953 - $15.00 USD Received 8 Jun 2007; revised 16 Aug 2007; accepted 23 Aug 2007; published 29 Aug 2007